Granular Matter (2011) 13:503–510
DOI 10.1007/s10035-011-0262-7

ORIGINAL PAPER

Numerical study on energy transformation in granular matter under biaxial compression

Zhongwei Bi · Qicheng Sun · Feng Jin · Ming Zhang

Received: 17 December 2010 / Published online: 31 March 2011

Abstract Granular matter consists of a large number of clearly distinguishable particles. Examples include coarse grain soil, rockfills and so on in which neighboring particles contact with each other and form skeletons to support gravity and other external loadings. Once the contacts are losing or re-creating, various kinds of energy, such as elastic energy, kinetic energy, would transform into each other, while some of them would dissipate if sliding occurs. In this paper, a biaxial test on a 2D granular sample is numerically simulated by using the software of PFC2D. The fluctuation of strain–stress relation is observed and considered as the stick-slip motion of force chain, i.e. destructing and re-constructing of force chain. Every kind of energy is calculated and analyzed at different stress–strain stages. They are further compared with force chain network configurations. It is found that as shear band fully developed, all the boundary work is almost dissipated within shear band. These findings emphasize the importance of study on mesoscale structure dynamics, such as particle and force chain re-arrangement.

Keywords Granular matter · Shear band · Energy analysis · Force chains

1 Introduction

Granular matter consists of individual particles. Typical size of particles spans from tens of micros to tens of meters which are usually encountered in coarse granular soil and debris flows. In many engineering problems, it's usually treated as a continuum medium with certain mechanical properties, but the continuum assumption would develop into an obstacle against further progress as soon as stress or strain localization (shear bands) occurs around a peak stress, and the shear bands would cause granular matter failure. As the initial constitutive model cannot well predict the appearance of shear bands, detailed studies have been conducted in the past few decades, and many improved models and theories are proposed, such as gradient plasticity theory, bifurcation theory and so on [1]. Especially, the non-localized damage model considers the microscopic structure of the materials, such as the interaction between the strain gradient and micro-cracks. The traditional mechanical model of localized damage is extended to non-local damage mechanics model, i.e. the stress of one point is not only related to its strain change history, but also affected by the interaction of material points in a certain neighborhood [2].

A large number of tests and simulations show that the macro properties of granular matter are affected by the micro fabric and properties. Oda [3] and Oda and Kazama [4] have observed the microstructure of shear bands developed in several natural sands by means of X-ray application and an optical method using a microscope and thin sections. Even there are extensive studies on shear bands and micro fabric, the micro-deformation mechanism leading to the development of shear bands is not yet well understood, and more importantly, the strain localization is still a hot topic in the theoretical as well as experimental study on the mechanics of granular materials.

In order to further study the effect of micro fabric to the mechanical properties of granular matter, an alternative to these continuous approaches is to use discrete-based methods which represent the material by an assemblage of independent elements (also called units, particles or grains), which interact with one another. The commonly adopted numerical method for discrete system is the particle flow code (PFC)

Z. Bi (✉) · Q. Sun · F. Jin · M. Zhang
State Key Laboratory of Hydroscience and Engineering, Tsinghua University, Beijing 100084, China
e-mail: bizhongwei1976@163.com

which is particularly suitable to simulate granular materials. It abandons the assumption of the continuum from the beginning and considers the matter as a conglomeration of discrete particles. It starts from the contacts among particles which obeys the contact law, such as Hook's linear contact law or Hertz's nonlinear contact law. It has been extended to solid mechanics to investigate the failure process of geomaterials, like rock [5,6] and concrete [7]. Nowadays, huge data of particle motion could be easily obtained in experiments and discrete element simulations, and complicated behaviors could be well understood from the view point of particle motion. For example, it is clear that shear band behavior is caused by strong particles' sliding and rotating. However, it's still a very hard issue that how to use the appropriate theory to explain or successfully predict the formation and development of the shear bands in granular matter [8].

By observing the shearing failure, it is found that the influence range of shearing is only limited to several times of particle size, while the particles beyond this range is almost free from shear effects [9]. Recent studies emphasize the importance of force chains, which is formed by quasi-linearly aligned particles. These quasi-linear structures bear and transmit the compressive loading on the system. The persistence of a force chain could resist the repulsive contact forces that push particles apart and try to break the chain. The transverse contact force is the main reason to break the chain, applied by particles belonging to weak chains. According to Albert's study about the resistance of slow movement objects in granular system, it can be concluded that the resistance is from a series of particle force chains in different depths [10]. The force chain intensity is different in different layers of the granular system, the deeper of the depth, and the more stable of the force chain. Evenly splitting the granular system along the direction of the shear bands to n-particle layer with a thickness, the force chain in each layer is corresponded to a critical force chain friction. When the applied stress is greater than the critical value, the force chain will deform, destruct or reconstruct, giving rise to the damage of force chain network, and the internal particles will relatively slide and rotate, and cause the energy loses. Tordesillas et al. [11] has studied the force chains' buckling process and established the relations between stability and energy of particle samples. Liu CS has conducted further research to the energy dissipation and decay properties of granular matter [12].

The high-frequency acoustic waves are often used in the above-mentioned experiments, but few experiments about the frequency response under low-frequency shear have been reported yet [13]. However, in Geotechnique engineering, the shear bands always appear in the loading process under quasi-static condition. Therefore, the study on the elastic energy, kinetic energy and so on of the whole granular system is very important for the study of the deformation of granular matter in the state of biaxial compression [14].

In this paper, the macro and micro mechanical behavior of the granular sample under biaxial compression is simulated with the software of PFC2D, the transformation of elastic energy, kinetic energy, energy dissipation as well as the evolution of energy with force chains are discussed, which is a try to explain the mechanical mechanism of granular matter from both energy and meso-structure view.

2 Simulation setup

Numerical simulations using the discrete element method (DEM) have become a valuable tool in the study of different phenomena occurring at the micro- and meso-mechanical scale in granular materials [15–18]. The mechanical response of the media is obtained by modeling the particle interactions as a dynamic process and using simple mechanical laws in these interactions. In this paper, simulations of biaxial test are used to investigate the behavior of granular materials. A 2D granular sample with 0.2 m high and 0.1 m wide is selected. It consists of 4325 round particles. Particle size obeys a uniform probability distribution in the range of 0.0046–0.0075 m. Surface friction coefficient $\mu = 0.5$, normal and tangential stiffness are both 5.0×10^8 N/m. Time step is $\Delta t = 10^{-6}$ s and the gravity is set to 0. The initial configuration is isotropic. To achieve this, each assembly is prepared by first dropping the particles into the container under a gravitational field, with the friction coefficient between particles set to zero. The assembly is then allowed to settle to a state where the kinetic energy is negligible, before it is compressed under an initial confining pressure. The isotropic assembly is then subjected to boundary driven biaxial compression. Simulations are performed under conditions of zero gravity. The assembly is compressed at a constant strain rate 0.1 mm/s in the vertical direction of the top boundary and bottom boundary. During the loading process, a constant confining pressure of 2, 1.5 and 1 MPa are applied in the horizontal direction. The deviatoric stress $\sigma = \sigma_1 - \sigma_3$, in which σ_1 is the axial stress, σ_3 is the level of confining pressure (Fig. 1). Axial strain is ε and the volumetric strain is ε_v.

Forces in a granular matter are transmitted via a two-phase network of contact forces: a strong contact force network comprising of the so-called 'force chains', which bear the majority of the loading; surrounding this is the complementary weak network of particles that provides lateral stability to the force chains (Fig. 1). At this time, the ring force chains are dominated in the granular matter and more uniformly distributed in spatial.

During the tests, the loading speed is required to be slow enough, so as to ensure the test is conducted in a quasi-static condition. It is very important to ensure the quasi-static defor-

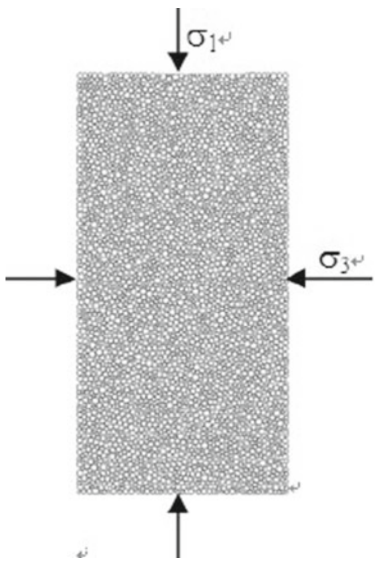

Fig. 1 Snapshot of a granular simulation sample (*left*); force chain network about $\sigma 3 = 2\,\text{MPa}$ (*right*)

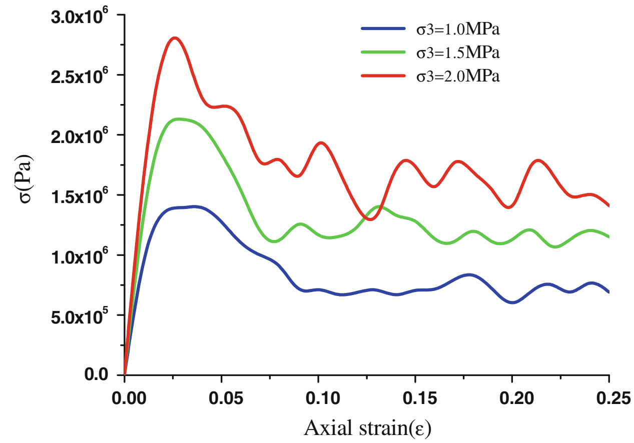

Fig. 2 The results for the partial stress versus axial strain

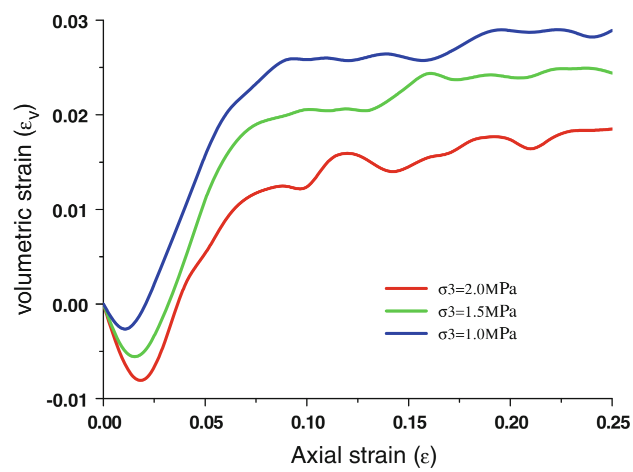

Fig. 3 The results for the volumetric strain versus axial strain

mation process. If the loading process is in dynamic condition rather than quasi-static one, the force chain behavior and movement of particles will demonstrate a very different behavior [19], which is not mentioned in the past studies or ignored. This paper analyzes the loading process under quasi-static condition, which can be checked by the boundary work compared with the elastic energy in the granular sample. If both are equal in the elastic part, which means it satisfies the quasi-static condition. Otherwise, the loading is in dynamic condition.

Figure 2 shows the deviatoric stress curve of granular system when σ_3 is 2, 1.5 and 1 MPa respectively. This observation matches Kruyt and Marroquin's observation [20,21]. It can be seen from Fig. 2, although the confining pressure is different, the deviatoric stress curve under three cases is almost overlapped in the elastic stage. Then the granular system enters into the plastic phase, and reaches the maximum peak strength; the peak strength are different under different confining pressures, but the ratio of the peak strength and confining pressure is ≈1.5, which indicates that the peak strength of granular system has nothing to do with confining pressure. Subsequently, the granular system enters into the softening stage and eventually the residual phase. In the residual phase, the ratio of the residual strength and confining pressure is ≈0.75. In this stage, the granular system shows very large fluctuations, which are considered as earthquake process by many scholars [22], and as stick-slip process by other ones [23], and thoroughly analyzed by combing jamming-unjammed process. The stick-slip phenomenon will be detailedly described in other papers.

In Fig. 3, the volume change of a typical simulation shows first compression, then dilatancy, and eventually a very weak change at very large deformations. Figure 3 shows that with the increase in confining pressure, the dilatancy of the granular matter is reduced i.e. confining pressure has a significant effect on the reduction in dilatancy of a granular assembly. This observation matches the results in [21]. Since the results are very similar, the energy analysis in the following will mainly focus on $\sigma_3 = 2\,\text{MPa}$. At the same time, when the axial strain of granular system reaches 15%, the volume strain has no big changes, and the granular system enters into stable flow state. The energy analysis on the stable flow state has been conducted by extensive literatures [24], so only when $\varepsilon \le 15\%$ is considered in this paper.

Figure 4 shows the stress–strain curves and the evolution of force chains. One reason for the large stress–strain fluctuation is from the scale effect, i.e. the number of particles of 4325 is not large enough. Another major reason is from the stick-slip motion of force chain network [23]. Force chains are self-adaptive under external loadings, i.e. the configuration of force chains transforms instantaneously into an appropriate stable state. If an applied force is large enough

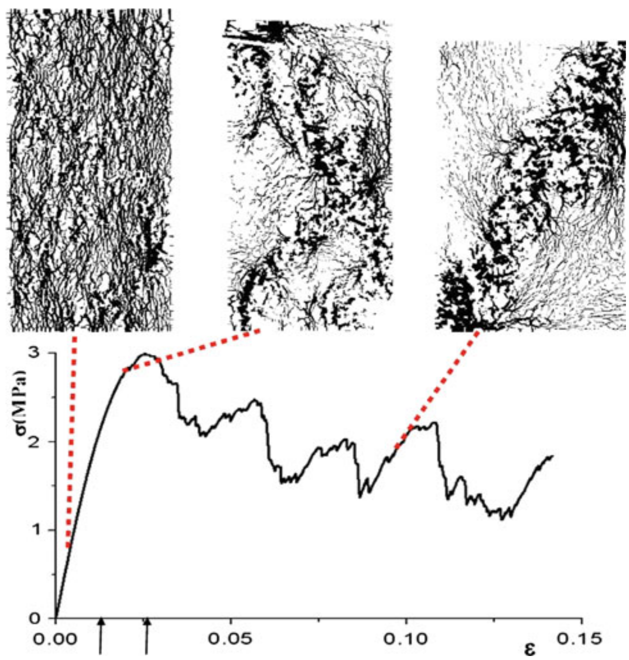

Fig. 4 The curve of stress with strain and three diagrams of force chain network transformation. Each diagram shows the difference of force chain during a time step of 10^{-6} s

to cause larger force chain configuration, a sudden drop in the stress of the granular system would be caused, as shown in the above stress–strain relation. We can see the frequent transformation of force chain configuration from the right inset, even within a short duration of 10^{-6} s. The problem of how to characterize the stick-slip motion of force chain network is open.

The two arrows in Fig. 4 from left to right respectively represent the starting point of elastic and plastic stage. This can be determined by the subsequent kinetic energy and friction energy pulse. From the stress–strain curve, we can see that the granular system experiences a complete elastic-plastic process. When $\varepsilon \approx 1.9\%$, the system shows significant elastic properties. With the increase of the axial strain, the system enters into the plastic stage, and the localized shear bands emerge. Initially, these localized shear bands (called microbands [25,26]) are very small and randomly distribute within the whole granular system. With the further increase of the axial strain, the localized shear bands begin to deliver, combine and form a number of distinct shear bands, and form an X-type shear band at some time. When $\varepsilon = 2.8\%$, the granular system achieves the peak strength, and subsequently with a rapid decline in stress. A single shear band appears along the direction of around 45°, and then the granular system enters into the softening stage and the residual stress stage.

It can be also observed by the force chain changes in Fig. 4. At different stress–strain stages, the force chain changes are not the same. When the loading is imposed to the top and bottom boundary, the vertical direction changes to the major principal stress direction, while the horizontal direction changes to the minor principal stress direction; then the force chain structure changes immediately into columns which are parallel to the vertical direction, i.e. the major principal stress direction. At the elastic stage, the force chain evolution mainly shows the thickening of the force chain and some of the sliding cracks which are evenly distributed in the granular system. With the system entering into the plastic stage, the evolution of force chains mainly shows a large number of dispersed shear sliding short force chains. When the shear bands are formed, the evolution of the force chains mainly centralizes in the shear bands, and the changes are mainly the formation and destruction of the force chains in the shear direction. At the same time, the number density of force chains inside of shear bands is significantly sparser than the one outside, and the force chain inside is significantly weaker than the one outside.

3 Energy analysis

In the shear failure under biaxial compression, there exists the following several main energy forms: the elastic energy, kinetic energy and frictional energy dissipation. Each of them will be analyzed one by one in the following. As to energy loss, there are two main types in granular systems. One type is the energy dissipation caused by mutual collisions between particles, which are usually defined by the camping coefficient. In this paper, the particle is defined as completely elastic collision, i.e. coefficient of restitution as 1, damping coefficient as 0. The other type is the energy dissipation caused by friction. One part of the particles loses contacts while another part of particles establishes new contacts by the external loading. Through these contacts changing, there exists energy dissipation, which is focused by this paper.

3.1 Elastic energy and critical sensitivity

The static loading method is used, so that at each stage the deformation is in equilibrium. Particle contact model is elastic, and the elastic energy is stored through the contact deformation of particle. The elastic energy formula is written in the below

$$E_e = \sum_{i=1}^{N_c} \left(\frac{|f^{cn}|^2}{2K_n} + \frac{|f^{ct}|^2}{2K_t} \right) \tag{1}$$

where N_c is the number of contacts. f^{cn} and f^{ct} are the normal force and tangential force, K_n and K_t are the normal stiffness and tangential stiffness. The results of E_e are shown in the inset of Fig. 5. From the fluctuation of E_e, we

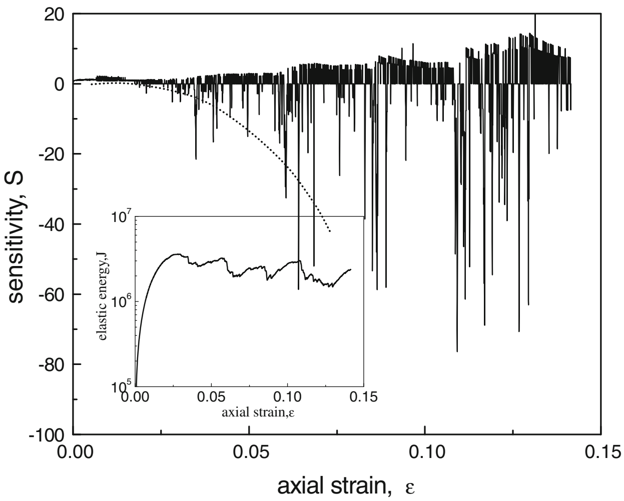

Fig. 5 Critical sensitivity in the biaxial test. The inset is the elastic energy. The dotted curve outlines the tendency of S. First a few sharp drops of S imply the following occurrence of shear bands

guess that the granular sample might become sensitive to axial strain prior to failure, i.e. critical sensitivity [27]. Since the controlling variable is the axial strain ε in the simulations, a sensitivity of elastic energy release to axial strain is defined by

$$S = \left(\frac{\Delta E_e}{\Delta \varepsilon}\right)\left(\frac{E_e}{\varepsilon}\right)^{-1} \tag{2}$$

where ΔE_e is the response of elastic energy release to axial strain increment $\Delta\varepsilon$. The sensitivity S is shown in Fig. 5.

From the inset of Fig. 5, it can be observed that the elastic energy curve is very similar with the stress–strain curve, indicating that when subjected to external loading, the granular system shows elastic effects, i.e. with the increase of stress, elastic energy also increases. The sensitivity S is shown in Fig. 2. Before $\varepsilon = 1.9\%$, S remains low and nearly a constant, indicating that in the elastic stage, the external loading is completely converted to elastic energy. This is easy to understand. When $\varepsilon = 1.9\%$, there is the first pulse of S, and then S increases and oscillates. The system begins the plastic deformation and the local force chains occur fracture and reorganization, combined with the subsequent pulses. Entering into the plastic stage, the granular sample dissipates energy due to plastic deformation. Since the ideal elastic particles are used in this simulation, the particle itself does not take place the plastic deformation, therefore, in this stage, the plastic energy is the energy caused by the unrecoverable structural changes of local force chains. When $\varepsilon = 2.8\%$, the elastic energy achieves the peak, i.e. the maximum energy storage of elastic energy. The cyclical fluctuation is closely linked to structural changes of the particles in the shear bands. At this stage, the sensitivity decreases very sharply ahead of eventual

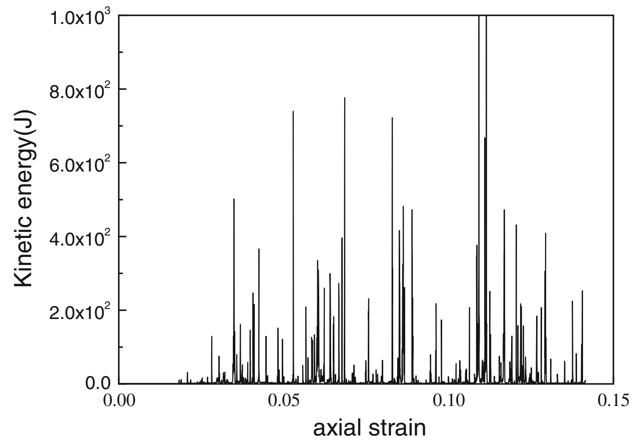

Fig. 6 Kinetic energy evolution

shear band appearance. So, it seems that critical sensitivity may provide a reasonable clue to shear band occurring.

3.2 Kinetic energy

Kinetic energy is mainly caused by the translation and rotation of particles in the process of breaking and restructuring of particle contacts. The variation of kinetic energy can be obtained by calculating the changes in particle velocity field, calculation formula is

$$E_c = \sum_{k=1}^{N} e_c^k \tag{3}$$

e_c^k is the kinetic energy variation of single particle

$$e_c^k = \frac{1}{2} m v^2 + \frac{1}{2} I \omega^2 \tag{4}$$

where m is the particle mass, v is the translational speed, I is the moment of inertia and ω is the rotational speed. Since the loading process in this work is under a quasi-static condition, the kinetic energy is as small as approximately 1% of the elastic energy, as shown in Fig. 6.

At the elastic and plastic stage, kinetic energy is close to zero due to the quasi-static loading of granular system. At the softening region and the residual phase, the kinetic energy shows large fluctuations. Combined the elastic energy shown in Fig. 5, the positions of kinetic energy incrementing exactly correspond to the positions of elastic energy decrease. It implies that the release of elastic energy first drive particles to move, and force chains consequently destruct and re-construct, and eventually the drop of elastic energy is largely transformed into plastic energy. When $\sigma_3 = 1.5$ and 1.0 MPa, the results are similar.

Literature [22] has conducted detailed analysis on the kinetic energy with the changing of time, and regarded the fluctuations of kinetic energy as earthquake process, which is very reasonable. While some other literature [23] regards the process as stick-slip process. The stick and slip events are periods where the stress increases and decreases, respectively, with increasing strain. A slip event is most often due to the collapse of force chains by buckling. In general, it is accompanied by the release of stored energy, accumulated in force chains during the preceding stick event. The force chain fracture will be particularly analyzed in Sect. 4.2.

3.3 Energy dissipation

According to Coulomb's law, when the friction force reaches the limit, the particles slide and rotate each other. The inter-rotating will not cause micro-deformation, so if all the particles rotate, there will be deformation without energy dissipation. When the system is under the quasi-static loading conditions, the stress anisotropy and contact network anisotropy in the granular system are not only because of the anisotropy of the contact force, but also because some particles are in sliding state, while the others are in rotating state.

The friction dissipation is the sliding energy dissipation of all contacts at a certain time step. Formula is written as

$$E_f = \sum_{N_c} \left((\langle f_i^s \rangle)(\Delta U_i^s)^{slip} \right) \tag{5}$$

where N_c is the number of particle contacts, F_i^s is the average shear stress, $(\Delta U_i^s)^{slip}$ is the sliding displacement incremental of the particle contacts at a certain time step. The sliding displacement incremental can be determined by the following formula

$$(\Delta U_i^s)^{slip} = \Delta U_i^s - (\Delta U_i^s)^{elas} = \Delta U_i^s + \frac{(\Delta f_i^s)^{elas}}{k^s} = \Delta U_i^s + \frac{(f_i^s)^{(t+\Delta t)} - (f_i^s)^{(t)}}{k^s} \tag{6}$$

In which, ΔU_i^s is the shear displacement incremental, composed by the elastic displacement $(\Delta U_i^s)^{elas}$ and sliding displacement, specified in the manual of PFC software. Figure 7 shows the dissipated energy due to friction sliding in the loading process. We can see that there is a roughly linearship between E_f and ε axial strain. It will be discussed in Sect. 4.1.

The distribution of number of sliding particles could roughly represent the distribution of energy dissipation in granular sample. From the inset in Fig. 7, we can see that energy dissipation mainly occur within shear bands, in which particles frequently slide. It is very necessary to conduct detailed study on force structure change and particle re-arrangement.

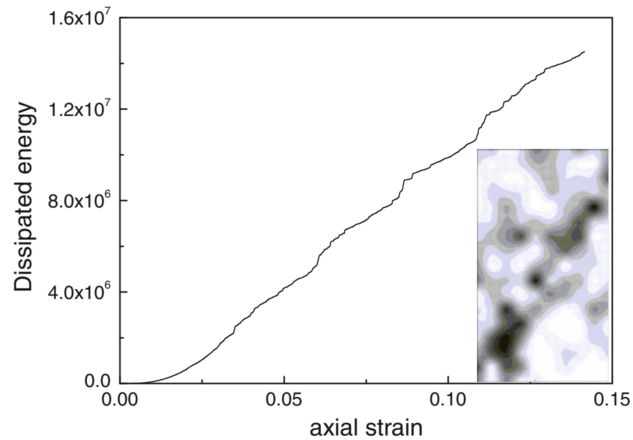

Fig. 7 Dissipated energy evolution. The inset is the contour of the number of sliding particles. Darker area corresponds to more particles' sliding

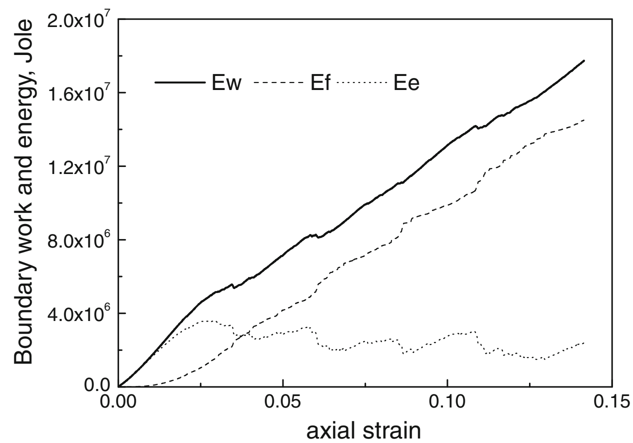

Fig. 8 Comparison of boundary work, dissipated energy and elastic energy

4 Discussions

4.1 Proportions of various kinds of energy

It is necessary to calculate the boundary work done by all walls on the granular sample. The total accumulated work E_w is written as

$$E_w \leftarrow E_w - \sum_{N_w} (F_i \Delta U_i + M_3 \Delta\theta_3) \tag{7}$$

where N_w is the number of walls; F_i and M_3 are the resultant force and moment acting on the wall at the start of the current timestep, and ΔU_i and $\Delta\theta_3$ are the applied displacement and rotation occurring during the current timestep. Note that this is an approximation in that it assumes that F_i and M_3 remain constant throughout the timestep. Also note that E_w may be positive or negative, with the convention that work done by the walls on the particles is positive.

Fig. 9 Force chains destruct and reconstruct within the shear band. Thicker chains represent stronger forces

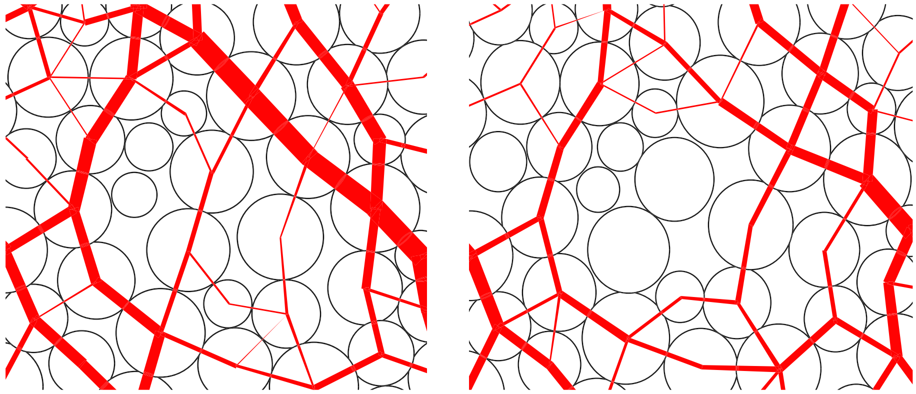

(a) Before fracture **(b)** After fracture

In Fig. 8, the boundary work E_w, elastic energy E_e and dissipated energy E_f are compared.

It can be observed from Figs. 5 and 8, with the increasing of axial strain, when the sample is in the elastic stage ($\varepsilon < 1.9\%$), E_w is almost fully converted into E_e. At this time, the kinetic energy and friction energy account for a very small proportion. When entering into the elastic stage ($\varepsilon < 2.8\%$), more than 85% of E_w is converted into E_e, and almost 14% is converted into E_f, only around 1% is converted into kinetic energy. After entering into the softening stage and residual stage ($\varepsilon > 2.8\%$), E_w is almost fully converted into E_f. The two curve slopes of E_e and E_w are very close, which also shows that, the transformation of energy is concentrated in the shear bands at the residual stage, and the particles have intense reorganization, rotation and so on within the shear bands. At the same time, in the whole loading process, the proportion of kinetic energy is very small, which indicates that the translation of particles is only in a very small scale. When $\sigma_3 = 1.5$ and 1.0 MPa, the results are similar. The analysis to reorganization of the particles within the shear bands will be followed.

4.2 Rearrangements of particles and force chains

The elastic energy release is related to the structural changes of particle in the shear bands, as shown in Fig. 9.

Figure 9 is an optional force chain map before and after fluctuation of the stress. Compared the two force-chain networks, it can be seen that with the stress reduction, some force chains occur fractures, and then disappear. The related particles begin sliding and rotating, so the corresponding kinetic energy also increases. At the same time, new force chains will be formed very fast. The speed is presumed close to the sound velocity. The transition of old force chains to new force chains corresponds to the jumps in stress. It is necessary to develop the high spatial and temporal resolution related testing technology in order to conduct site, real-time observation and capture in this process.

From Fig. 9, we also can see that in the hardening process up to failure, particles are arranged in chains to form column-like structures whose elongation directions are more or less parallel to the major principal stress axis, and the applied stress is mainly transmitted through them. During the process, the pre-existing contacts are lost in the minor principal stress direction, but rather some contacts are newly formed in the major principal stress direction. As a result, an elongated void is generated between two neighboring columns. This is the micro-mechanism leading to dilatancy before failure.

5 Outlook

Various kinds of energy have different proportions at different stress–strain stages. At both elastic and plastic stages, the boundary work is mainly converted into elastic energy. In the following stage of residential stage, frequent particle sliding and topological changes of force chains become stronger, and almost all the boundary work is dissipated. More importantly, the energy dissipation is mainly localized in a narrow shear band.

It should be noted that, the macro-shear bands are formed through the cascade, combination and development of micro-shear bands, which implies a very complex process. The paper only has a discussion from the energy point of view. Further studies are going to be conducted on the particle and force chain re-arrangement by means of high speed camera and photoelastic technique.

Acknowledgments The authors acknowledge the support of the National Key Basic Research program of China (No.: 2010CB731504), the National Natural Science Foundation of China (No.: 50904036; 11034010) and the research funding from the State Key Laboratory of Hydroscience and Engineering, Tsinghua University (No.: 2008-ZY-6; 2010-TC-1).

References

1. Calvetti, F., Combe, G., Lanier, J.: Experimental micromechanical analysis of a 2D granular material: relation between structure evolution and loading path. Mech. Cohes. Frict. Mater. **2**(1), 121–163 (1997)
2. Bi, Z.W., Zhang, M., Jin, F.: Non-local damage and fracture model of rock and concrete-like materials. Trans. Nonferrous Met. Soc. China **19**(s3), 824–828 (2009)
3. Oda, M.: A micro-deformation model for dilatancy of granular materials. In: Symposium on Mechanics of Particulate Materials in McNu Conference, ASCE, pp. 24–37 (1997)
4. Oda, M., Kazama, H.: Micro-structure of shear band and its relation to the mechanism of dilatancy and failure of granular soils. Geotechnique **48**(4), 465–481 (1998)
5. Hajiabdolmajid, V., Kaiser, P.K., Martin, C.D.: Modeling brittle failure of rock. Int. J. Rock Mech. Min. Sci. **39**(6), 731–741 (2002)
6. Potyondy, D.O., Cundall, P.A.: A bonded particle model for rock. Int. J. Rock Mech. Min. Sci. **41**(8), 1329–1364 (2004)
7. Hentz, S., Daudeville, L., Donze, F.V.: Identification and validation of a discrete element model for concrete. J. Mech. Eng. **130**(6), 709–719 (2004)
8. Wan, R.G., Guo, P.J.: Stress dilatancy and fabric dependencies on sand behavior. J. Eng. Mech. **130**(6), 635–645 (2004)
9. Cundall, P.A., Strack, O.D.L.: Discrete numerical model for granular assembles. Geotechnique **29**(1), 47–65 (1979)
10. Albert, R., Pfeifer, M.A., Barabasi, A.L.: Slow drag in a granular medium. Phys. Rev. Lett. **82**(1), 205–208 (1999)
11. Tordesillas, A., Walker, D.M., Lin, Q.: Force cycles and force chains. Phys. Rev. E **81**, 011302 (2010)
12. Tordesillas, A.: Force chain buckling, unjamming transitions and shear banding in dense granular assemblies. Philos. Mag. **87**(32), 4987–5016 (2007)
13. Wang, P.J., Li, Y.D., Xia, J.H., Liu, C.S.: Characterization of reflection intermittency in a composite granular chain. Phys. Rev. E **77**, 060301 (2008)
14. Zhao, Z., Liu, C.S.: Energy dissipation and dispersion effects in granular media. Phys. Rev. E **78**, 031307 (2008)
15. Kadau, D., Schwesig, D., Theuerkauf, J. et al.: Influence of particle elasticity in shear testers. Granul. Matter **8**(1), 35–40 (2006)
16. Sazzad, M.M., Suzuki, K.: Micromechanical behavior of granular materials with inherent anisotropy under cyclic loading using 2D DEM. Granul. Matter **12**(6), 597–605 (2010)
17. Luding, S.: Anisotropy in cohesive, frictional granular media. J. Phys. Condens. Matter **17**(24), S2623–S2640 (2005)
18. Mohamed, A., Gutierrez, M.: Comprehensive study of the effects of rolling resistance on the stress–strain and strain localization behavior of granular materials. Granul. Matter **12**(5), 527–541 (2010)
19. Cafiero, R., Luding, S., Herrmann, H.J.: Two-dimensional granular gas of inelastic spheres with multiplicative driving. Phys. Rev. Lett. **84**(26), 6014–6017 (2000)
20. Luding, S.: Shear flow modeling of cohesive and frictional fine powder. Powder Technol. **158**(1-3), 45–50 (2005)
21. Alonso-Marroquin, F., Muhlhaus, H.B., Herrmann, H.J.: Micromechanical investigation of soil plasticity using a discrete model of polygonal particles. Theor. Appl. Mech. **35**(1-3), 11–28 (2008)
22. Tillemans, H.-J., Herrmann, H.J.: Simulating deformations of granular solids under shear. Phys. A **217**(3-4), 261–288 (1995)
23. Ciamarra, M.P., Lippiello, E., Godano, C., Arcangelis, L.d.: Unjamming dynamics: the micromechanics of a seismic fault model. Phys. Rev. Lett. **104**, 238001 (2010)
24. Roeck, M., Morgeneyer, M., Schwedes, J. et al.: Steady state flow of cohesive and non-cohesive powders: investigations in experiment and simulation. Granul. Matter **10**(4), 285–293 (2008)
25. Kuhn, M.R.: Structured deformation in granular materials. Mech. Mater. **31**(6), 407–429 (1999)
26. Antony, S.J., Kuhn, M.R.: Influence of particle shape on granular contact signatures and shear strength: new insights from simulations. Int. J. Solids Struct. **41**(21), 5863–5870 (2004)
27. Zhang, X.H., Xu, X.H., Wang, H.Y. et al.: Critical sensitivity in driven nonlinear threshold systems. Pure Appl. Geophys. **161**(9-10), 1931–1944 (2004)